Nrf2 protects against cartilage endplate degeneration through inhibiting NCOA4-mediated ferritinophagy

ZHENKAI MA[1], HUI LU[1], XUEMIN FENG[2], TING DU[3], JIANHUA LI[1], QIANG ZHANG[1], XINDONG GU[1], YUANDONG SHAO[4], XINGZHI JING[5] and CHENG SU[5]

Departments of [1]Neurosurgery and [2]Endocrinology, Binzhou People's Hospital, Binzhou, Shandong 256600; [3]Department of Medicine, Yidu Cloud (Beijing) Technology Co., Ltd., Beijing 100191; [4]Department of Spine Surgery, Binzhou People's Hospital, Binzhou, Shandong 256600; [5]Department of Spine Surgery, Shandong Provincial Hospital Affiliated to Shandong First Medical University, Jinan, Shandong 250000, P.R. China

Received July 19, 2023; Accepted November 12, 2023

DOI: 10.3892/ijmm.2023.5339

Abstract. Iron overload and ferroptosis are associated with intervertebral disc degeneration (IDD); however, the mechanism underlying the regulation of iron homeostasis remains to be elucidated. Nuclear factor erythroid 2-related factor 2 (Nrf2) has been reported to regulate cellular iron homeostasis; however, its impact on IDD pathology and the underlying mechanism of action requires further investigation. In the present study, immunohistochemistry analysis of Nrf2 expression in the cartilage endplate (CEP) was conducted and it was demonstrated that Nrf2 expression was increased in the CEP at the early stages of the development of IDD, whereas it was decreased at the late stages of the development of IDD. The results of western blot analysis indicated that the inadequate activation of Nrf2 may aggravate mitochondrial dysfunction and oxidative stress, thus promoting CEP chondrocyte degeneration and calcification. It was also revealed that Nrf2 was involved in TNF-α-induced CEP chondrocyte iron metabolism dysfunction and ferroptosis. Inhibition of Nrf2 expression using Nrf2 small interfering RNA could enhance the process of nuclear receptor coactivator 4 (NCOA4)-mediated ferritinophagy and increase ferrous ion content, which may promote CEP chondrocyte ferroptotic cell death and extracellular matrix degradation. Furthermore, a decrease in cellular iron concentration may inhibit CEP chondrocyte ferroptosis, and CEP degeneration and calcification. The present study highlights the role of the Nrf2/NCOA4 axis in chondrocyte ferroptosis and IDD pathogenesis, thus suggesting that activation of Nrf2 may be a promising strategy for IDD treatment.

Correspondence to: Dr Cheng Su, Department of Spine Surgery, Shandong Provincial Hospital Affiliated to Shandong First Medical University, 324 Jingwu Weiqi Road, Jinan, Shandong 250000, P.R. China
E-mail: spinesc0405@163.com

Dr Yuandong Shao, Department of Spine Surgery, Binzhou People's Hospital, 515 Huanghe Seven Road, Binzhou, Shandong 256600, P.R. China
E-mail: syd201213@126.com

Abbreviations: CEP, cartilage endplate; NP, nucleus pulposus; AF, annulus fibrosus; LIP, labile iron pool; IDD, intervertebral disc degeneration; ROS, reactive oxygen species; Nrf2, nuclear factor erythroid 2-related factor 2; GPX4, glutathione peroxidase 4; NCOA4, nuclear receptor coactivator 4; GSH, glutathione; FTH, ferritin heavy chain; FPN, ferroportin; DFO, desferoxamine

Key words: Nrf2, NOCA4, CEP, ferritinophagy, IDD

Introduction

Chronic low back and leg pain originating from intervertebral disc degeneration (IDD) affects daily life, and is the main cause of adult disability, thus resulting in a substantial economic burden to society and families (1). Due to the increase in the elderly population and an increase in sedentary lifestyles, the number of patients with IDD-related diseases has been continuously increasing (2). The intervertebral disc is the largest avascular tissue in the human body, and its nutritional supply is received mainly via diffusion through the cartilage endplate (CEP) and annulus fibrosus (AF). The CEP is the main route for this nutrition supply, with 75% of normal intervertebral disc nutrition originating from infiltration in this region (3). Studies have shown that aging and degenerative changes in the CEP can significantly affect the biomechanics and nutritional supply status of the intervertebral disc, and are considered to be the initiating factors leading to IDD (1,4). Chondrocytes are the only cell type in the CEP, which synthesize and secrete extracellular matrix to maintain the structure and function of the vertebral CEP. Normal adult chondrocytes are terminally differentiated cells and cannot adapt to microenvironmental changes through self-renewal (5). Concomitantly, the CEP lacks nerve and vascular distribution, which disables its ability to react to pathological conditions. Therefore, excessive mechanical stress, inflammation and metabolic abnormalities may lead to oxidative stress damage or even death of chondrocytes, which in turn can lead to degeneration and calcification of the CEP (6).

The transcription factor nuclear factor erythroid 2-related factor 2 (NFE2L2/Nrf2) was initially identified as a central controller of cellular redox homeostasis (7). Nrf2 is normally continuously ubiquitinated and degraded when bound to Kelch-like ECH-associated protein 1 (Keap1) in the cytoplasm. However, following induction of oxidative or electrophilic stress in the cell, the spatial conformation of Keap1 is altered, enabling the release of Nrf2 from Keap1 and its translocation to the nucleus. This in turn activates target genes, including those involved in the cell antioxidant response and regulation of iron homeostasis, lipid metabolism and mitochondrial function regulation (8). Controlled activation of Nrf2 in normal cells serves important roles in redox balance. By contrast, the inhibition or insufficient activation of Nrf2 is associated with the onset of oxidative stress. Oxidative stress has been demonstrated to be the leading cause of IDD. The protective effect of various phytochemicals extracted from plants, such as astaxanthin or icariin, against the development of IDD is attributed to the activation of Nrf2 signaling (9,10). However, to the best of our knowledge, only one study has assessed the roles of Nrf2 in CEP degeneration (11).

Iron is the largest trace element in the human body, and it participates in a wide range of physiological functions and biochemical reactions. However, excessive iron can lead to the production of a large number of reactive oxygen species (ROS) by participating in electron transfer of the mitochondrial respiratory chain, which can lead to the destruction of mitochondrial structure and the disruption of mitochondrial function, as well as the induction of oxidative stress, lipid peroxidation and DNA damage; these events eventually lead to iron-dependent programmed ferroptosis (12). Previous studies have shown that the accumulation of iron in tissues and cells is a common feature in a series of degenerative diseases, including IDD (13,14). Recent studies have shown that iron overload and ferroptosis can lead to oxidative stress injury and the death of chondrocytes, which are important factors contributing to articular cartilage degeneration (15,16) and IDD (17,18). As a result, the pursuit of targeting ferroptosis has emerged as a potential therapeutic strategy for these diseases. However, the regulatory mechanism of iron metabolism in CEP chondrocytes under pathological conditions requires further investigation.

In the present study, the regulatory effects of Nrf2 and its role in CEP chondrocyte degeneration were explored with regard to cellular iron homeostasis and ferroptosis. The present study aimed to offer insights into the involvement of the Nrf2 pathway and iron homeostasis in the pathogenesis of CEP degeneration. The ultimate goal was to assess the potential of developing effective therapeutic strategies for inhibiting the progression of IDD.

Materials and methods

Primary CEP chondrocyte isolation and culture. A total of 20 C57BL/6J male mice (age, 5 days) were anesthetized by intraperitoneal injection of 2% pentobarbital sodium (35 mg/kg body weight) and sacrificed via cervical dislocation. All animals were purchased from the Experimental Animal Center of Shandong First Medical University and maintained in ventilated filter-top cages under standard laboratory conditions at a constant temperature of 25˚C and 40% humidity under a 12-h light/dark cycle, and were given free access to conventional rodent chow with water. All animal protocols were approved by the Institutional Animal Care Committee of the Shandong Provincial Hospital Affiliated to Shandong First Medical University (approval no. 2022-816; Jinan, China). The tissues were minced into small pieces using a dissecting microscope, and were then incubated with 0.25% trypsin (Gibco; Thermo Fisher Scientific, Inc.) for 30 min and with 0.25% type 2 collagenase (MilliporeSigma) for 4-6 h at 37˚C. Chondrocytes were harvested following centrifugation at 250 x g for 10 min at room temperature and were resuspended in DMEM/F12 (Gibco; Thermo Fisher Scientific, Inc.) supplemented with 10% fetal bovine serum (FBS; Gibco; Thermo Fisher Scientific, Inc.), 1% streptomycin sulfate and 1% penicillin. The cells were cultured in an incubator maintained with 5% CO_2 at 37˚C. The culture medium was changed every other day.

siRNA transfection. siRNAs targeting Nrf2 and a negative control siRNA were synthesized by Guangzhou RiboBio Co., Ltd. The siRNA sequences were as follows: Nrf2#1, sense 5'-CCACCGCCAGGACTACAGT-3'; Nrf2#2, sense 5'-GATGGACTTGGAGTTGCCA-3'; Nrf2#3, sense 5'-CAGGACTACAGTCCCAGCA-3'; scrambled siRNA, sense 5'-TTCTGCGAACGAGTGACGT-3' and antisense 5'-ACCTGACGCGTACGGAGAA-3'. When cells reached 60-70% confluence, they were transfected with 50 nM siRNA using Lipofectamine® 3000 (cat. no. L3000015; Invitrogen; Thermo Fisher Scientific, Inc.) for 5 h at 37˚C. The negative control group was transfected with scrambled siRNA. Subsequently, the medium was replaced with normal growth medium comprised of DMEM/F12 and 10% FBS. A total of 1 day post-transfection, chondrocytes were used for further study.

Western blot analysis. CEP chondrocytes were treated with 0, 0.1, 1, 5 and 10 ng/ml of TNF-α (R&D Systems, Inc.) with or without Nrf2 small interfering RNA (siRNA) or 100 μM desferoxamine (DFO; cat. no. D9533; MilliporeSigma) for 24 h at 37˚C. Then, cells were lysed with RIPA buffer (cat. no. CW2333; CoWin Biosciences) supplemented with a protease inhibitor cocktail for 15 min on ice; subsequently, total protein was collected following centrifugation at 2,500 x g at 4˚C for 20 min. The concentration of total protein was measured using the bicinchoninic acid assay protein assay kit (Beyotime Institute of Biotechnology). A total of 25 μg total protein was added and subsequently subjected to separation by SDS-PAGE on 10% gels, followed by the transfer of the separated proteins onto polyvinylidene difluoride membranes (MilliporeSigma). After blocking with 5% BSA (Wuhan Boster Biological Technology, Ltd.) for 30 min at room temperature, the membranes were incubated with primary antibodies against Nrf2 (cat. no. 16396-1-AP; 1:1,000; Proteintech Group, Inc.), heme oxygenase (HO)-1 (cat. no. BM4010; 1:1,000; Wuhan Boster Biological Technology, Ltd.), nuclear receptor coactivator 4 (NCOA4; cat. no. ab86707; 1:1,000; Abcam), LC3B (cat. no. 4108; 1:1,000; Cell Signaling Technology, Inc.), dynamin-related protein 1 (Drp1; cat. no. 12957-1-AP; 1:1,000; Proteintech Group, Inc.), mitochondrial fission factor (MFF; 1:1,000; cat. no. 84580; Cell Signaling Technology,

Inc.), ferritin heavy chain 1 (FTH1; cat. no. ab75973; 1:1,000; Abcam), type II collagen (COL2; cat. no. 28459-1-AP; 1:1,000; Proteintech Group, Inc.), SOX9 (cat. no. A00177-2; 1:500; Wuhan Boster Biological Technology, Ltd), Parkin (cat. no. 14060-1-AP; 1:1,000; Proteintech Group, Inc.), matrix metalloproteinase (MMP)3 (cat. no. 17873-1-AP; 1:1,000; Proteintech Group, Inc.), MMP13 (cat. no. 18165-1-AP; 1:1,000; Proteintech Group, Inc.), solute carrier family 7 member 11 (SLC7A11; cat. no. 26864-1-AP; 1:1,000; Proteintech Group, Inc.), COL10 (cat. no. BA 2023; 1:500; Wuhan Boster Biological Technology, Ltd.), mitochondrial fission 1 (FIS1; cat. no. 10956-1-AP; 1:1,000; Proteintech Group, Inc.), RUNX2 (cat. no. PB0171; 1:500; Wuhan Boster Biological Technology, Ltd.), glutathione (GSH) peroxidase 4 (GPX4; cat. no. 67763-1-Ig; 1:1,000; Proteintech Group, Inc.) and GAPDH (cat. no. 10494-1-AP; 1:2,000; Proteintech Group, Inc.). Following an overnight incubation at 4˚C, the membranes underwent three washes with TBS-0.1% Tween 20. The membranes were subsequently incubated with the corresponding horseradish peroxidase-conjugated anti-rabbit or anti-mouse secondary antibodies (1:2,000; cat. nos. BA1061 and BA1062; Wuhan Boster Biological Technology, Ltd.) for 1 h at room temperature. The signal intensity of the membranes was visualized with enhanced chemiluminescence reagent (Wuhan Boster Biological Technology, Ltd.) and images were captured using a Bio-Radscanner (Bio-Rad Laboratories, Inc.).

Immunofluorescence staining. CEP chondrocytes were isolated and seeded onto a 12-well plate. The cells were subsequently subjected to 5 ng/ml TNF-α treatment with or without Nrf2 siRNA when reaching 80% confluence. Following fixation at room temperature for 20 min with 4% paraformaldehyde and permeabilization with 0.1% Triton X-100 (cat. no. T8787; Sigma-Aldrich; Merck KGaA), the cells were blocked with 5% BSA (Wuhan Boster Biological Technology, Ltd.) for 1 h at room temperature and incubated with primary antibodies against COL2 (cat. no. 28459-1-AP, 1:500; Proteintech Group, Inc.), GPX4 (cat. no. 67763-1-lg; 1:200; Proteintech Group, Inc.) and NCOA4 (cat. no. ab86707; 1:500; Abcam) at 4˚C overnight. Subsequently, the cells were incubated with Cy3-conjugated goat anti-rabbit secondary antibody (cat. no. A0516; Beyotime Institute of Biotechnology; 1:500) in the dark for 1 h at 37˚C. The cells were then subjected to a washing step with PBS and labeled with DAPI (cat. no. AR1177; Wuhan Boster Biological Technology, Ltd.) for 5 min with a fluorescence microscope (Olympus Corporation).

To examine the colocalization of mitochondria and Parkin, as well as Drp1, cells were incubated with diluted Mito-Tracker Red CMXRos solution (cat. no. C1049B; Beyotime Institute of Biotechnology) in the dark at 37˚C for 30 min. After MitoTracker incubation, cells were subjected to fixation and permeabilization as aforementioned, then the cells were incubated with Parkin (cat. no. 14060-1-AP; 1:200; Proteintech Group, Inc.) and Drp1 (cat. no. 12957-1-AP; 1:200; Proteintech Group, Inc.) antibodies at 4˚C overnight, and were then incubated with fluorescein isothiocyanate-conjugated goat anti-rabbit secondary antibodies (cat. no. A0562; Beyotime Institute of Biotechnology; 1:500) in the dark at 37˚C for 1.5 h. After washing with PBS and labeling with DAPI, fluorescence microscopy (Axio Observer 3; Carl Zeiss AG) was employed to capture the images and detect the differences in the fluorescence expression of the corresponding proteins.

Assessment of intracellular ROS and mitochondrial membrane potential. The primary cause of oxidative stress in IDD is the excessive accumulation of ROS. To assess intracellular ROS production, a Reactive Oxygen Species Assay Kit (cat. no. S0033; Beyotime Institute of Biotechnology) was used, according to the manufacturer's instructions. The CEP cells were subjected to three washes with serum-free medium. Subsequently, dichloro-dihydro-fluorescein diacetate was diluted to 10 μM in serum-free medium and added to the cells for 30 min at 37˚C in the dark. After washing the cells with serum-free medium, they were examined under a fluorescence microscope (Axio Observer 3; Carl Zeiss AG).

Mitochondrial membrane potential was evaluated using a mitochondrial membrane potential kit (cat. no. C2006; Beyotime Institute of Biotechnology). Briefly, after incubation with the JC-1 staining working solution for 20 min at 37˚C, CEP chondrocytes were rinsed with ice-cold JC-1 washing buffer three times. Multimeric JC-1 with red fluorescence transitions to monomeric JC-1 with green fluorescence, thus indicating the loss of mitochondrial membrane potential. The changes in mitochondrial membrane potential were captured using an inverted fluorescence microscope (Axio Observer A1; Carl Zeiss).

Alizarin red staining. Briefly, chondrocytes derived from the CEP were seeded in 24-well plates at a density of $1x10^5$ cells/well. The osteogenic differentiation culture medium (Cyagen Biosciences, Inc.) was added to the cells when cell confluence reached 80%, and the cells were incubated for 3 weeks at 37˚C. After thorough rinsing with PBS and fixation with 4% paraformaldehyde at room temperature for 20 min, the cells were stained with alizarin red solution (Cyagen Biosciences, Inc.) at room temperature for 30 min. Semi-quantification of the mineralized nodules was achieved using spectrophotometric analysis. Specifically, following dissolution in 10% (wt/vol) cetylpyridinium chloride (Sigma-Aldrich; Merck KGaA) for 1 h at room temperature, semi-quantification was performed by measuring its optical density at 570 nm.

Ferrous ion (Fe^{2+}) detection. Chondrocytes were seeded in a 24-well plate at a concentration of $1x10^5$ cells/ml. After 1 day, serum-free medium containing 5 ng/ml TNF-α was added to the cells and they were cultured for 24 h. Subsequently, medium was replaced with serum-free medium containing 0.1 mmol/l ammonium ferric citrate (MilliporeSigma) and cells were cultured for 2 h. After three washes with Hank's Balanced Salt Solution (HBSS; Wuhan Boster Biological Technology, Ltd.), the cells were stained with 1 μM FerroOrange (Dojindo Laboratories, Inc.) in HBSS for 40 min at 37˚C. Subsequently, the cells underwent three additional washes with HBSS and were then subjected to imaging using a fluorescence microscope (Axio Observer 3; Carl Zeiss AG).

Mitochondrial-specific fluorescence staining. Mito-Tracker Green (Beyotime Institute of Biotechnology) was employed to assess the morphological changes of mitochondria. Following

treatment of the cells with 5 ng/ml TNF-αfor 24 h at 37˚C, they were rinsed twice with FBS-free DMEM/F12, and then exposed to FBS-free DMEM/F12 and incubated with diluted Mito-Tracker Green solution (1:1,000) for 30 min at 37˚C in the absence of light. Subsequently, the images were captured using a fluorescence microscope (Axio Observer 3; Carl Zeiss AG).

Immunohistochemical (IHC) analysis. To examine the expression pattern of Nrf2 in aging mice, 20 3-week-old C57/BL6 male mice (weight, 10 g) were randomly divided into the following groups: 1, 3, 6 and 16 months (n=5/group), and were maintained in ventilated filter-top cages under standard laboratory conditions at a constant temperature of 25˚C and 40% humidity under a 12-h light/dark cycle, and were given free access to conventional rodent chow with water. C57/BL6 mice were purchased from the Experimental Animal Center of Shandong Provincial Hospital Affiliated to Shandong First Medical University. At the age of 1, 3, 6 and 16 months, mice were anesthetized by an intraperitoneal injection of 2% pentobarbital sodium (35 mg/kg body weight) and were sacrificed via cervical dislocation. Subsequently, L4/5 intervertebral disc samples were collected and fixed in 4% paraformaldehyde at 4˚C for at least 24 h. To perform IHC analysis, the following steps were executed: The samples underwent deparaffinization using xylene, followed by blocking with 5% BSA-containing PBS solution for 30 min at 37˚C. After antigen retrieval in citrate buffer at 100˚C for 30 min, the sections were incubated with primary antibodies against Nrf2 (cat. no. 16396-1-AP; 1:200; Proteintech Group, Inc.) overnight at 4˚C. The samples were then incubated with biotinylated donkey anti-rabbit secondary antibodies (cat. no. BA1002; Wuhan Boster Biological Technology, Ltd.) at room temperature for 30 min. Finally, the sections were incubated for 10 min with 3,3'-diaminobenzidine at room temperature and counterstained with hematoxylin at room temperature for 5 min. Images were captured under a microscope (EVOS FL Auto system; Thermo Fisher Scientific, Inc.) and Image Pro Plus software (version 6.0; Media Cybernetics) was used to analyze the images of IHC staining. At least five randomly selected cartilage fields were used to accurately count immune-positive cells, and the percentage of immune-positive cells relative to the overall number of cells was calculated. The animals were treated and used in accordance with all applicable international, national and institutional guidelines.

Statistical analysis. Data are presented as the mean ± SD. All analyses were performed with GraphPad Prism software (version 9.0; Dotmatics). Comparisons between multiple groups were analyzed using one-way ANOVA followed by Tukey's test. For data that were expressed as a relative fold change and for comparisons between the control group and each of the treatment groups, a one-way ANOVA with Dunnett's test was performed. $P<0.05$ was considered to indicate a statistically significant difference.

Results

IDD is characterized by altered expression of Nrf2 and mitochondrial dysfunction. Aging is the leading cause of IDD (19). As shown in Fig. 1A and B, degenerated CEP with bony tissues that contained bone marrow and mineralized bone were observed in mice that were >3 months old. Furthermore, IHC analysis indicated that Nrf2 expression was higher in the degenerated CEP when compared with the CEP in 1-month old mice and the highest expression of Nrf2 was observed in 3-month-old mice. The expression of Nrf2 in the CEP was decreased after 3 months and no significant difference was noted between the CEPs derived from 1-month-old and 16-month-old mice. To further determine the expression pattern of Nrf2 during CEP degeneration, TNF-α was used to mimic endplate osteochondritis; the protein expression levels of Nrf2 and those of its downstream protein heme oxygenase (HO)-1 were increased following treatment with TNF-α, and were decreased when the TNF-α concentration reached >1 ng/ml, which was similar to the results obtained from the *in vivo* experiments (Fig. 1C and D). These results indicated that a low dose of TNF-α could activate a Nrf2-mediated antioxidant effect. To mimic the pathological condition in cartilage osteochondritis, a higher concentration of TNF-α (5 ng/ml) was used in the present study.

Nrf2 serves essential roles in redox homeostasis and mitochondrial function (20). To determine the function of Nrf2 in CEP chondrocytes under endplate osteochondritis conditions, the production of ROS and the development of mitochondrial dysfunction were examined. As shown in Fig. 1E, TNF-α treatment markedly promoted ROS production. Subsequently, JC-1 staining was utilized to investigate the collapse of the mitochondrial membrane potential. As shown in Fig. 1F, the ratio of green JC-1 monomers to red JC-1 aggregates was increased in the TNF-α treatment group, indicating the collapse of mitochondrial membrane potential. Mitochondria in healthy chondrocytes displayed a normal shape. As shown in Fig. 1G-K, TNF-α treatment markedly promoted mitochondrial destruction with increased expression levels of the mitochondrial fission proteins, MFF and Drp1. Also the mitophagy protein Parkin was slightly increased in response to a low dose of TNF-α (<5 ng/ml) and was significantly decreased when TNF-α reached 10 ng/ml. In addition, the immunofluorescence analysis of the mitochondria indicated the destruction of mitochondria with the presence of short and granulated mitochondria. These results indicated a negative association between Nrf2 and CEP degeneration. During the late stage of IDD development, Nrf2 expression was downregulated alongside excess ROS production and mitochondrial dysfunction.

TNF-α impairs iron homeostasis and promotes ferroptosis. Ferroptosis plays important roles in the development of IDD (21). In the present study, the labile iron pool (LIP) and the expression levels of ferroptosis markers were examined in CEP chondrocytes following TNF-α treatment. As shown in Fig. 2A and B, TNF-α significantly increased the immunofluorescence intensity of the Fe^{2+} probe, indicating that it promoted the Fe^{2+} levels of the LIP. Subsequently, the expression levels of the ferroptosis markers, GPX4, SLC7A11 and FTH1 were examined. Western blot analysis indicated that the expression levels of GPX4, a key factor of ferroptosis, were significantly reduced by TNF-α; similarly, the expression levels of FTH and SLC7A11 were reduced (Fig. 2C-D, F-G). The decreased

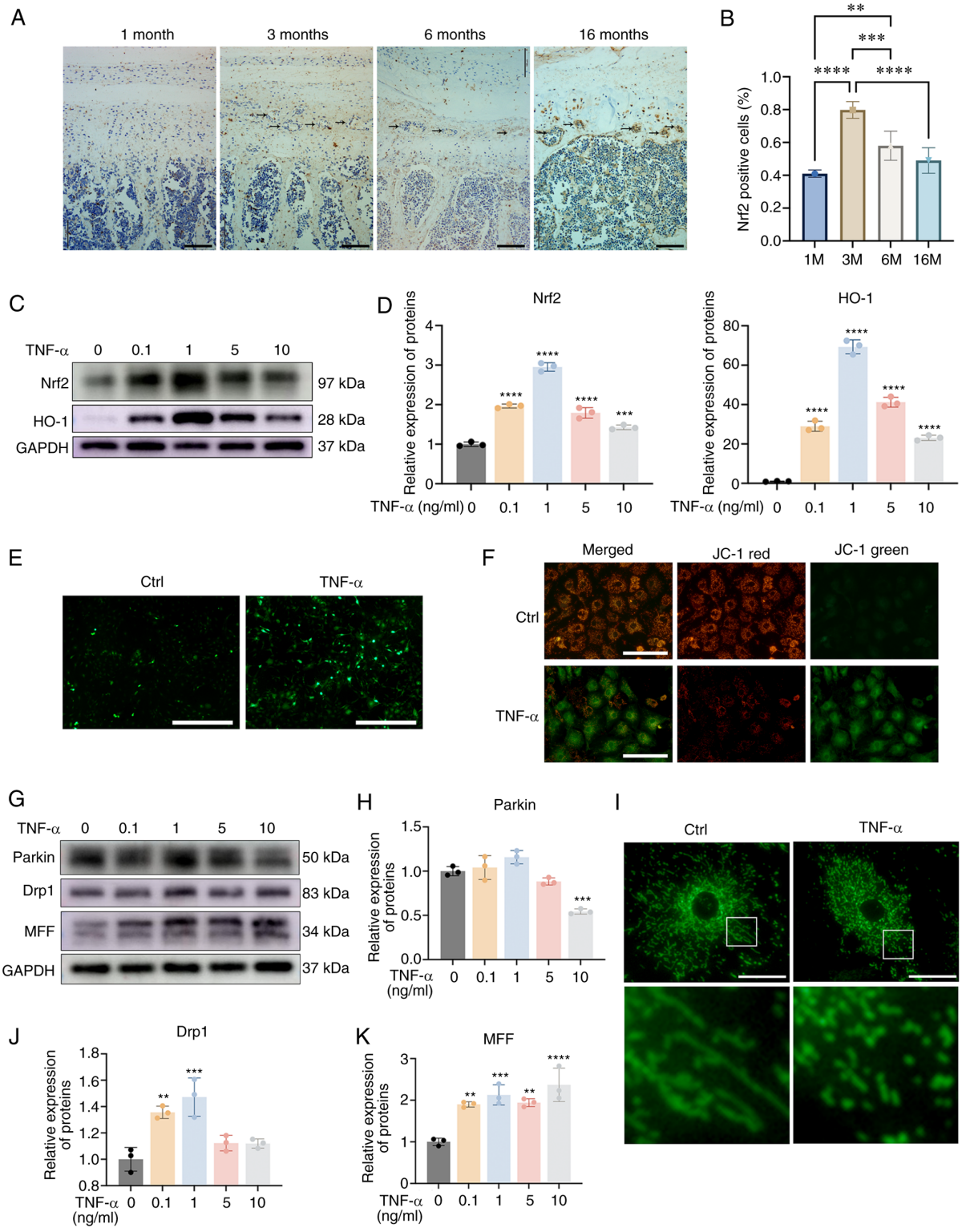

Figure 1. IDD is characterized by altered expression of Nrf2 and mitochondrial dysfunction. (A) Immunohistochemistry for Nrf2 in the CEP from mice aged 1, 3, 6 and 16 months. Black arrows indicate bony tissues. Scale bar, 100 μm; magnification, x200. (B) The ratio of Nrf2-positive cells was determined under a microscope using five sections from seven mice. (C) CEP chondrocytes were treated with increasing concentrations of TNF-α for 24 h, and western blotting was conducted to examine the protein expression levels of Nrf2, HO-1 and GAPDH. (D) The band density was semi-quantified and normalized to the control. (E) CEP chondrocytes were treated with 5 ng/ml TNF-α for 24 h, and representative fluorescence photomicrographs of intracellular ROS in chondrocytes are shown. Scale bar, 400 μm. (F) Representative fluorescence photomicrographs of mitochondrial membrane potential following incubation with JC-1. Red fluorescence was emitted by JC-1 aggregates in healthy mitochondria with polarized inner mitochondrial membranes, whereas green fluorescence was emitted by cytosolic JC-1 monomers, indicating mitochondrial membrane potential collapse. Scale bar, 200 μm. (G) CEP chondrocytes were treated with increasing concentrations of TNF-α for 24 h, and western blotting was conducted to examine the protein expression levels of Parkin, Drp1 and MFF. The band density of (H) Parkin was semi-quantified and normalized to the control. (I) Representative fluorescence images of mitochondria. CEP chondrocytes were treated with 5 ng/ml TNF-α for 24 h and the morphology of the mitochondria was visualized using Mito-Tracker Green staining. Scale bar, 25 μm. The band density of (J) Drp1 and (K) MFF was semi-quantified and normalized to the control. Data are presented as the mean ± SD from three independent experiments. **P<0.01, ***P<0.001, ****P<0.0001 vs. 0 ng/ml TNF-α group or as indicated. CEP, cartilage endplate; Ctrl, control; Drp1, dynamin-related protein 1; HO-1, heme oxygenase-1; MFF, mitochondrial fission factor; Nrf2, nuclear factor erythroid 2-related factor 2.

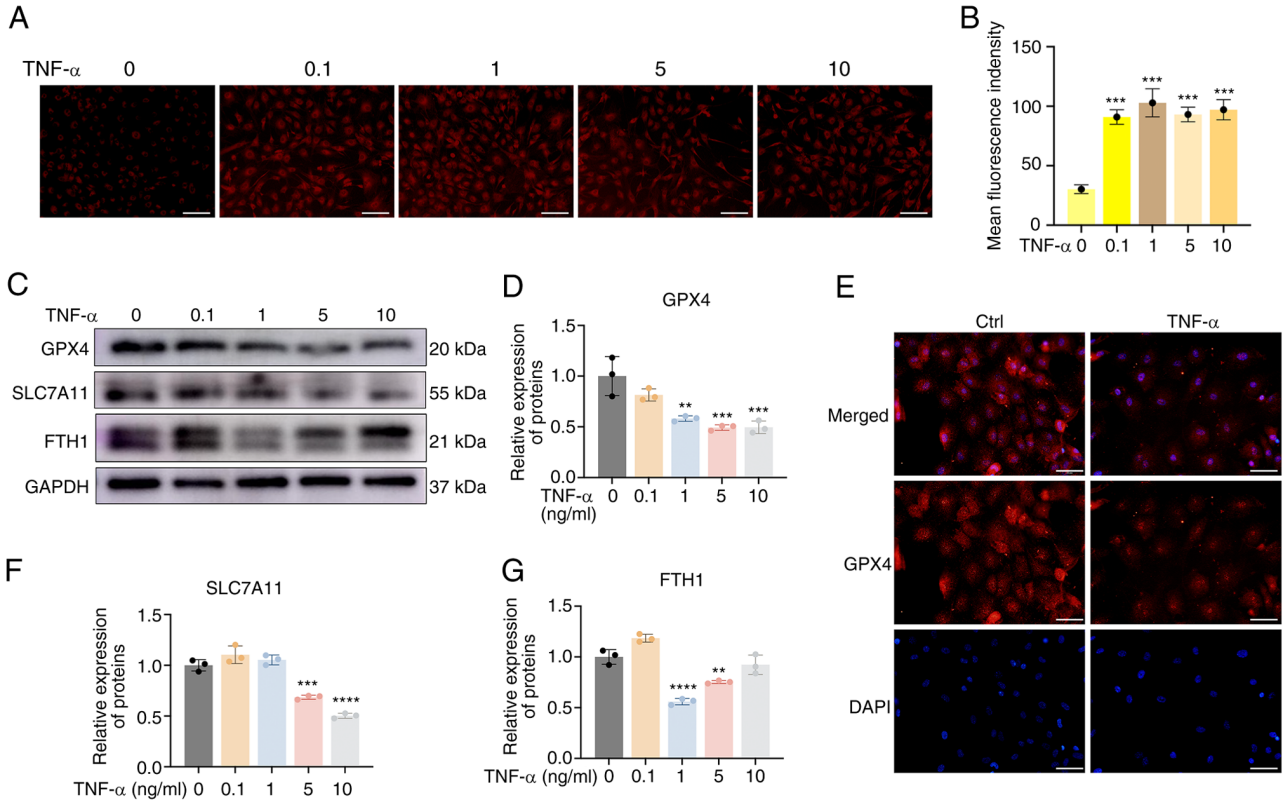

Figure 2. TNF-α impairs iron homeostasis and promotes ferroptosis. (A) CEP chondrocytes were treated with increasing concentrations of TNF-α with 100 μM ammonium ferric citrate for 20 min. Representative staining of Fe^{2+} is shown. Scale bar, 100 μm. (B) Statistical analysis of fluorescence intensity (Fe^{2+}) is shown. (C) CEP chondrocytes were treated with increasing concentrations of TNF-α for 24 h, and western blotting was conducted to examine the protein expression levels of GPX4, SLC7A11 and FTH1. (D) Band density of GPX4 was semi-quantified and normalized to the control. (E) CEP chondrocytes were treated with 5 ng/ml TNF-α for 24 h, and representative fluorescence photomicrographs of GPX4 in CEP chondrocytes are shown. Scale bar, 50 μm. The band density of (F) SLC7A11 and (G) FTH1 was semi-quantified and normalized to the control. Data are presented as the mean ± SD from three independent experiments. **P<0.01, ***P<0.001, ****P<0.0001 vs. 0 ng/ml TNF-α. CEP, cartilage endplate; Ctrl, control; Fe^{2+}, ferrous ion; FTH, ferritin heavy chain; GPX4, glutathione peroxidase 4; SLC7A11, solute carrier family 7 member 11.

GPX4, SLC7A11 and FTH1 expression indicated increased CEP chondrocyte ferroptosis. In addition, immunofluorescence analysis of GPX4 indicated a similar trend; the red fluorescence activity of GPX4 was decreased following TNF-α treatment (Fig. 2E). These results indicated that TNF-α could increase the Fe^{2+} levels of the LIP and promote ferroptosis.

Nrf2 inhibition sensitizes CEP chondrocytes to ferroptosis by promoting NCOA4-mediated ferritinophagy. NCOA4-mediated ferritinophagy has recently been demonstrated to serve important roles in regulating intracellular Fe^{2+} balance, and emerging evidence has reported that NCOA4 can regulate ferroptosis (22). The present study investigated whether NCOA4 was involved in CEP chondrocyte ferroptosis and whether NCOA4 was regulated by Nrf2. As shown in Fig. 3A, the protein expression levels of NCOA4 were upregulated in CEP chondrocytes following TNF-α treatment. Subsequently, Nrf2 siRNA was synthesized and transfected into CEP chondrocytes; the transfection efficiency was evaluated by western blot analysis and Nrf2#1 was used in subsequent experiments(Fig. 3D). The levels of Fe^{2+} and ferroptosis markers were then examined. As shown in Fig. 3B and E, inhibition of Nrf2 expression promoted the expression levels of NCOA4 and the amount of cellular Fe^{2+} when compared with the TNF-α group. Similar results of immunofluorescence analysis of NCOA4 were obtained, indicating that inhibition of Nrf2 further promoted CEP chondrocyte NCOA4 expression (Fig. 3E). JC-1 staining results indicated that inhibition of Nrf2 expression impaired the mitochondrial membrane potential, as demonstrated by the increased fluorescence levels of the JC-1 green probe and the decreased fluorescence levels of the JC-1 red probe (Fig. 3C). Compared with the TNF-α-treated group, inhibition of Nrf2 expression significantly enhanced the ferroptosis process, as determined by the reduced expression of ferroptosis markers, including GPX4, SLC7A11 and FTH (Fig. 3F and G). These results indicated that Nrf2 could inhibit the NOCA4-mediated ferritinophagy process and maintain cellular Fe^{2+} balance. Inhibition of Nrf2 expression enhanced NCOA4-mediated ferritinophagy and increased the levels of active Fe^{2+} of the LIP and sensitized CEP chondrocytes to ferroptosis.

Nrf2 inhibition aggravates CEP chondrocyte degeneration and calcification. To determine the role of Nrf2 in CEP degeneration and calcification, CEP chondrocytes were isolated and transfected with Nrf2 siRNA, and the role of the Nrf2/HO-1 axis in TNF-α-induced CEP degeneration and calcification was investigated. As shown in Fig. 4A and B, transfection of cells with Nrf2 siRNA further promoted TNF-α-induced CEP degeneration and matrix degradation, as indicated by increased

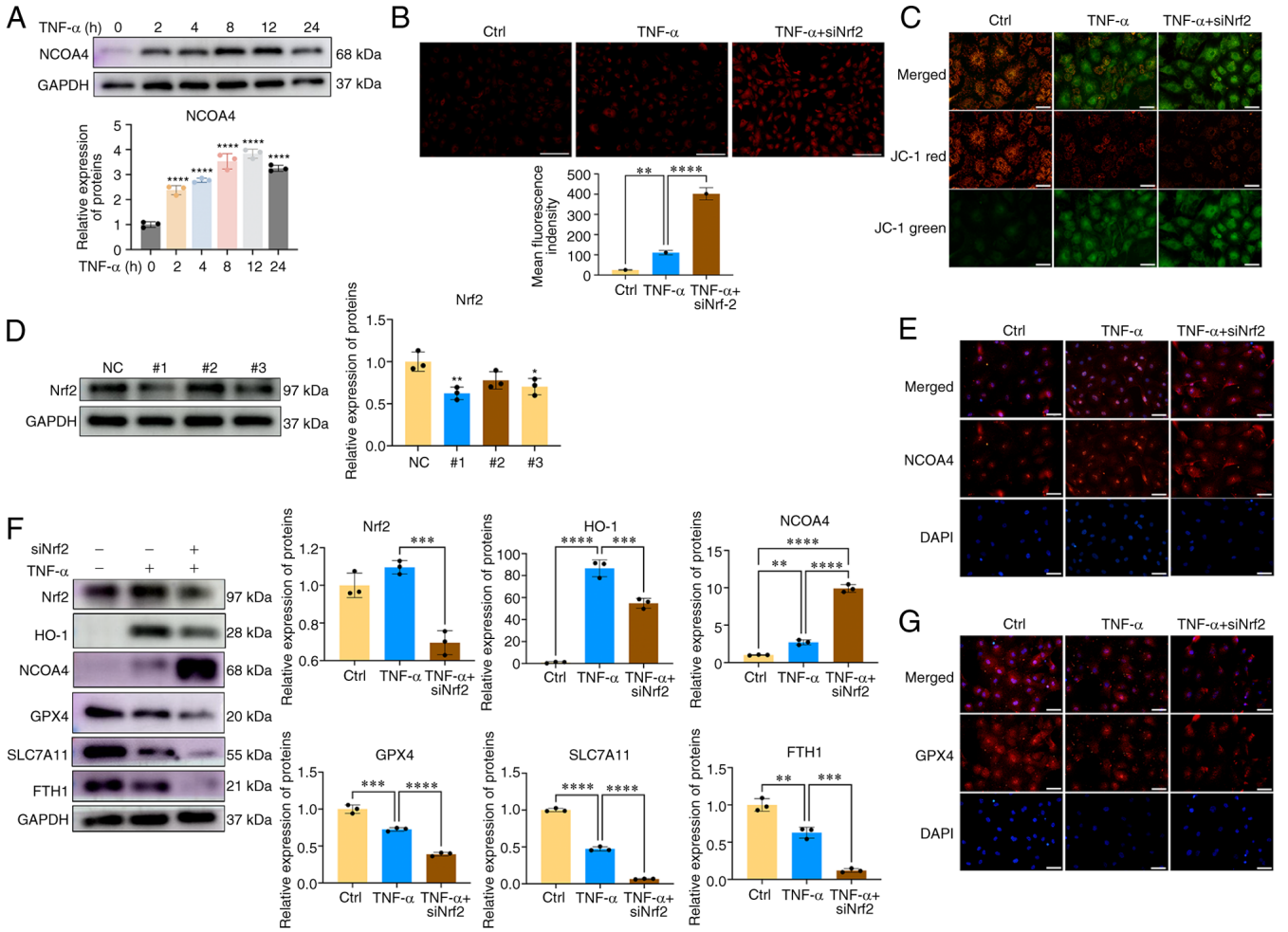

Figure 3. Nrf2 inhibition sensitizes CEP chondrocytes to ferroptosis via promoting NCOA4-mediated ferritinophagy. (A) CEP chondrocytes were treated with increasing concentrations of TNF-α for 24 h, and western blotting was conducted to examine the protein expression levels of NCOA4 and GAPDH. The band density was semi-quantified and normalized to the control. (B) CEP chondrocytes were treated with TNF-α with or without Nrf2 siRNA transfection. Representative staining for ferrous ions and statistical analysis of fluorescence intensity (ferrous ions) are shown. Scale bar, 200 μm. (C) Representative fluorescence photomicrographs of mitochondrial membrane potential after incubating with JC-1 in the indicated group are shown. Scale bar, 50 μm. (D) Transfection efficiency was evaluated by detecting Nrf2 expression using western blotting. (E) CEP chondrocytes were treated with TNF-α with or without Nrf2 siRNA transfection. Representative fluorescence microscopy photomicrographs of NCOA4 in CEP chondrocytes are shown. Scale bar, 50 μm. (F) CEP chondrocytes were transfected with Nrf2 siRNA and were then treated with 5 ng/ml TNF-α for 24 h. Western blotting was conducted to examine the protein expression levels of Nrf2, HO-1, NCOA4, GPX4, SLC7A11, FTH and GAPDH. The band density was semi-quantified and normalized to the control. (G) CEP chondrocytes were treated with TNF-α with or without Nrf2 siRNA transfection. Representative fluorescence microscopy photomicrographs of GPX4 in CEP chondrocytes are shown. Scale bar, 50 μm. Data are presented as the mean ± SD from three independent experiments. *P<0.05, **P<0.01, ***P<0.001, ****P<0.0001. CEP, cartilage endplate; Ctrl, control; FTH, ferritin heavy chain; GPX4, glutathione peroxidase 4; HO-1, heme oxygenase-1; NC, negative control; NCOA4, nuclear receptor coactivator 4; Nrf2, nuclear factor erythroid 2-related factor 2; siRNA, small interfering RNA; SLC7A11, solute carrier family 7 member 11.

MMP3, MMP13 and COL10 expression, and decreased SOX9 and COL2 expression when compared with the TNF-α group. Similar results were obtained by immunofluorescence analysis of COL2, indicating that Nrf2 siRNA further inhibited the red fluorescence staining of COL2 protein expression (Fig. 4C). Oxidative stress and iron overload can promote CEP chondrocyte osteogenic differentiation and calcification (23). As shown in Fig. 4D and E, inhibition of Nrf2 further promoted the formation of calcium nodules. These results demonstrated the essential role of Nrf2 in ameliorating CEP degeneration, and indicated that inhibition of Nrf2 expression could aggravate CEP chondrocyte degeneration and calcification.

Inhibition of Nrf2 results in mitochondrial dysfunction and decreased mitophagy. Mitochondrial dysfunction and the subsequent overproduction of ROS serve important roles in the development of IDD (24). It has been reported that Parkin activation can eliminate impaired mitochondria and ameliorate the progression of IDD (25). Next, CEP chondrocytes were transfected with Nrf2 siRNA before TNF-α co-treatment; scrambled siRNA was used as negative control. The expression levels of Parkin and changes in mitochondrial morphology were then investigated. As shown in Fig. 5A and C, the expression levels of Parkin in the 5 ng/ml TNF-α + siNC group were significantly increased when compared with those in the control group, while following inhibition of Nrf2 expression, the expression levels of Parkin and LC3B were inhibited, indicating that inhibition of Nrf2 decreased the mitophagy process. Double staining of Parkin and mitochondria indicated that Nrf2 siRNA reduced aggregation of Parkin in the mitochondria of TNF-α-stimulated CEP chondrocytes (Fig. 5B). In addition, the expression levels of the mitochondrial

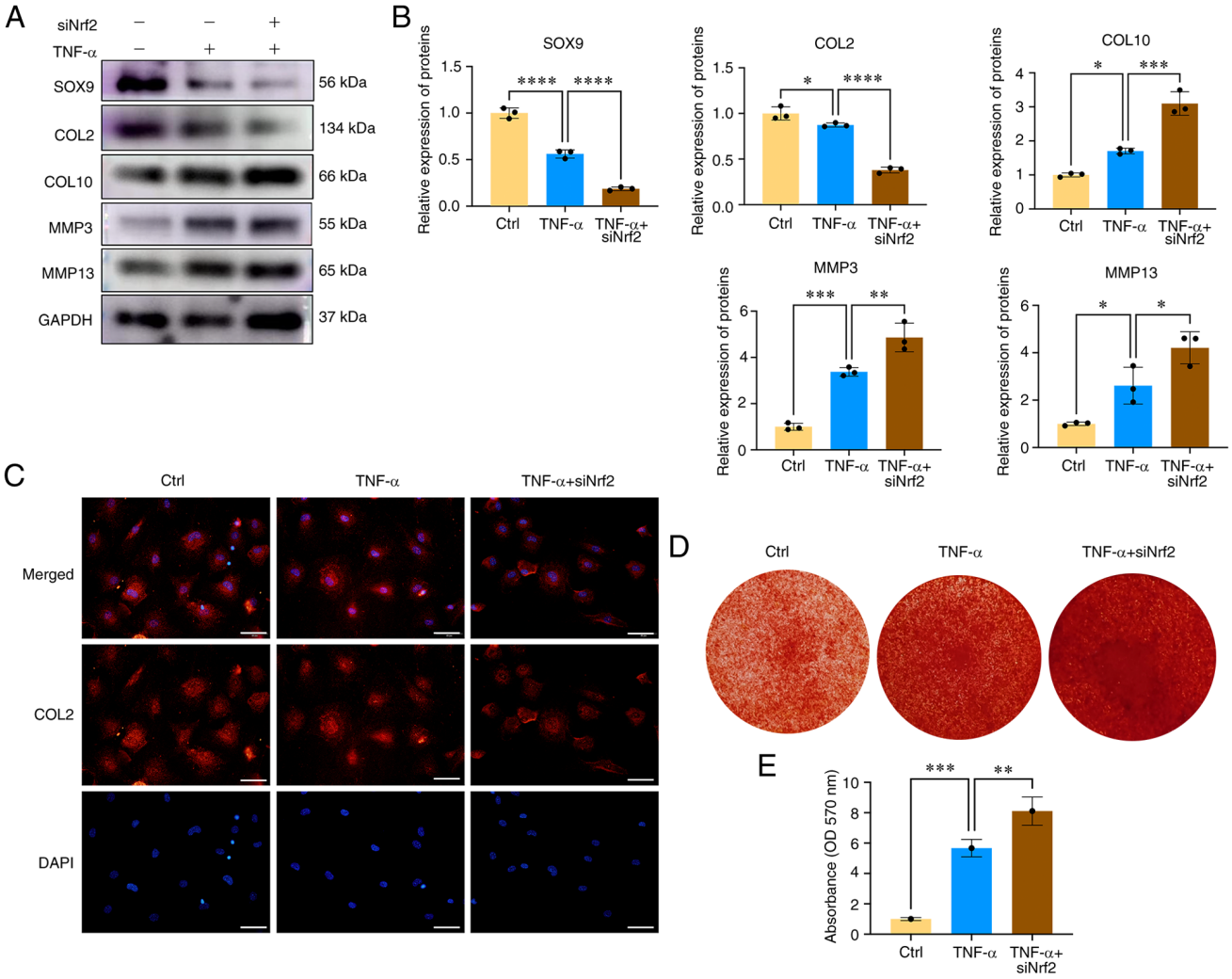

Figure 4. Nrf2 inhibition aggravates CEP chondrocyte degeneration and calcification. (A) CEP chondrocytes were transfected with Nrf2 siRNA and then treated with 5 ng/ml TNF-α for 24 h. Western blotting was conducted to examine the protein expression levels of SOX9, COL2, COL10, MMP3, MMP13 and GAPDH. (B) The band density was semi-quantified and normalized to the control. (C) CEP chondrocytes were treated with TNF-α with or without Nrf2 siRNA transfection. Representative fluorescence photomicrographs of COL2 in CEP chondrocytes are shown. Scale bar, 50 μm. (D) Alizarin Red staining for calcium deposition in CEP chondrocytes. (E) Semi-quantitative analysis of the mineralized nodules in CEP chondrocytes is shown. Data are presented as the mean ± SD from three independent experiments. *P<0.05, **P<0.01, ***P<0.001, ****P<0.0001. CEP, cartilage endplate; COL, collagen; Ctrl, control; MMP, matrix metalloproteinase; Nrf2, nuclear factor erythroid 2-related factor 2; siRNA, small interfering RNA.

fission proteins, including MFF, Drp1 and FIS1 were further increased by Nrf2 siRNA, which suggested the destruction of the mitochondrial morphology (Fig. 5A and C). As shown in Fig. 5D, immunofluorescence results indicated that Nrf2 siRNA further led to the destruction of mitochondrial morphology, with an increased number of short and granulated mitochondria. Moreover, elevated colocalization of Drp1 and mitochondria was observed in the Nrf2 siRNA treatment group. These results indicated that Nrf2 inhibition decreased CEP chondrocyte mitophagy and promoted mitochondrial dysfunction.

Iron chelation with desferoxamine (DFO) ameliorates CEP chondrocyte degeneration and calcification. Subsequently, the role of iron ions in CEP chondrocyte degeneration was assessed via DFO co-treatment. DFO can chelate iron ions and decrease the levels of cellular iron ions. As shown in Fig. 6A, TNF-α promoted CEP chondrocyte degeneration, which was accompanied by decreased expression levels of the chondrogenesis proteins SOX9 and COL2, and increased expression levels of cartilage matrix-degrading enzymes, including MMP3 and MMP13. However, co-treatment of cells with DFO and TNF-α reversed the detrimental effect of TNF-α, and was accompanied by increased expression levels of SOX9, and decreased levels of MMP3 and MMP13. Immunofluorescence of COL2 obtained similar results, in that DFO promoted COL2 protein expression (Fig. 6B). The degeneration and calcification of the CEP can significantly diminish the oxygen and nutrient supply to intervertebral discs, and is an important contributing factor in IDD. To explore the potential inhibitory effects of DFO on CEP calcification, and the expression of chondrocyte hypertrophic and osteogenic markers, including RUNX2 and COL10, western blot analysis was conducted. As shown in Fig. 6C, DFO exhibited a significant inhibitory effect on the expression levels of TNF-α-induced hypertrophic and osteogenic markers (COL10 and RUNX2). Furthermore, CEP chondrocytes were treated with DFO to determine its effects on chondrocyte osteogenic

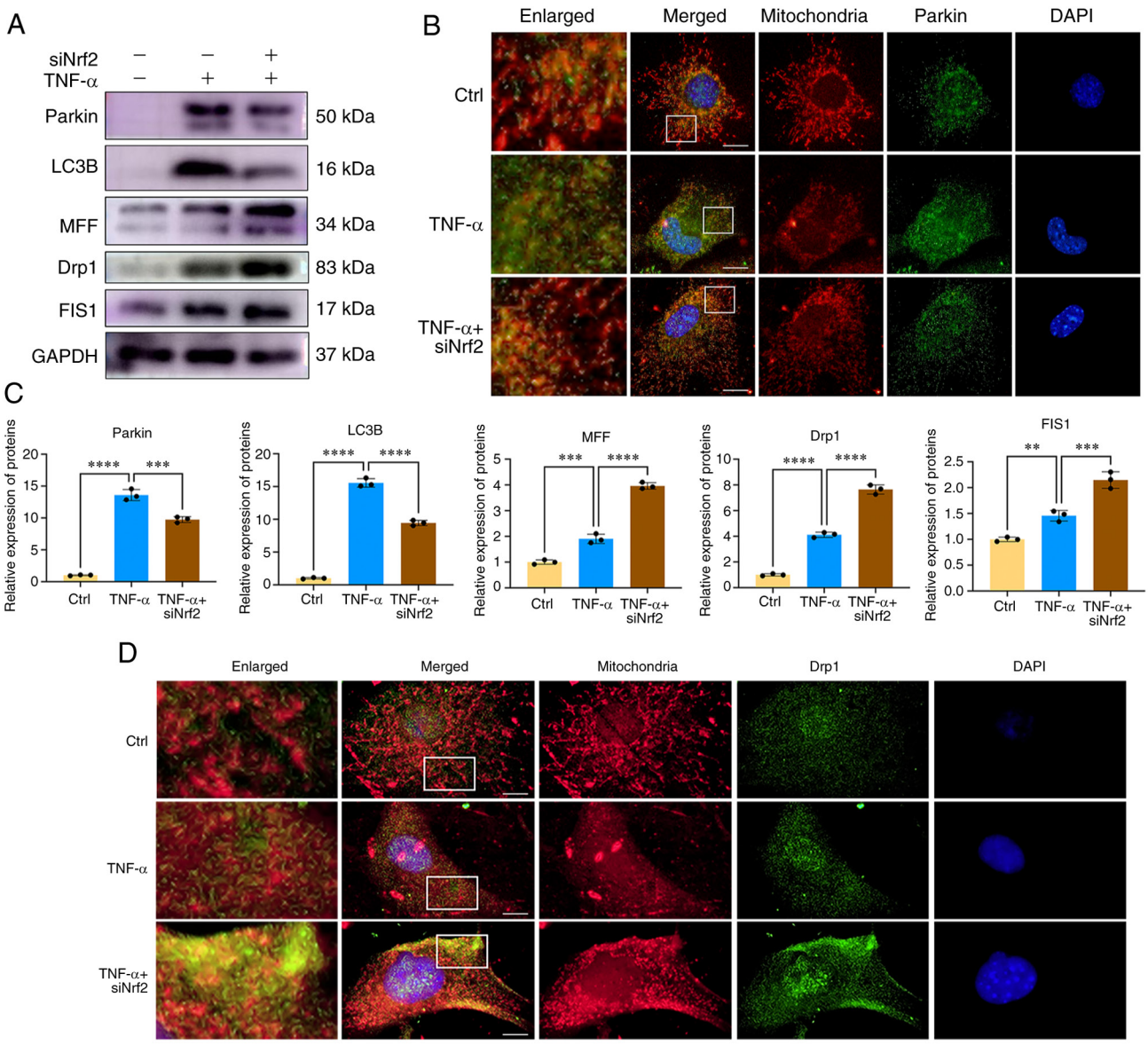

Figure 5. Nrf2 inhibition results in mitochondrial dysfunction and decreased mitophagy. (A) CEP chondrocytes were transfected with Nrf2 siRNA and then treated with 5 ng/ml TNF-α for 24 h. Western blotting was conducted to examine the protein expression levels of Parkin, LC3B, MFF, Drp1, MFF, FIS1 and GAPDH. (B) Immunofluorescence staining was conducted to examine the expression and localization of Parkin (green), mitochondria (red). Scale bar, 10 μm. (C) The band density was semi-quantified and normalized to the control. (D) Immunofluorescence staining was conducted to examine the expression and localization of Drp1 (green) and mitochondria (red). Scale bar, 10 μm. Data are presented as the mean ± SD from three independent experiments. **P<0.01, ***P<0.001, ****P<0.0001. CEP, cartilage endplate; Ctrl, control; Drp1, dynamin-related protein 1; FIS1, mitochondrial fission 1; MFF, mitochondrial fission factor; Nrf2, nuclear factor erythroid 2-related factor 2; siRNA, small interfering RNA.

differentiation and mineralization. Fig. 6D displays the results of alizarin red staining, which was used to assess calcium nodule formation. TNF-α treatment markedly promoted the formation of mineralized deposits in CEP chondrocytes, an effect that could be reversed following co-treatment of the cells with DFO and TNF-α. As shown in Fig. 6E, western blot analysis revealed that DFO treatment restored the diminished protein expression levels of GPX4 and SLC7A11 in CEP chondrocytes, indicating that DFO effectively inhibited TNF-α-induced CEP chondrocyte ferroptosis. These findings suggested that an excess of iron ions may contribute to CEP chondrocyte degeneration and calcification, and that reducing cellular iron ions represents an effective approach to inhibit CEP chondrocyte degeneration and calcification.

Discussion

The degeneration and calcification of the CEP can significantly hinder the nutrient supply to the intervertebral disc, making it a recognized and substantial contributor to the initiation and development of IDD (26). Although clinical evidence has established a close association between endplate osteochondritis and IDD, previous investigations have predominantly concentrated on the degeneration of the nucleus pulposus (NP) and AF; however, the mechanisms underlying CEP degeneration have not yet been fully elucidated (27). The strategy of targeting CEP degeneration aims to enhance nutrient and oxygen supply to the intervertebral disc, and is gaining increasing attention. It has previously

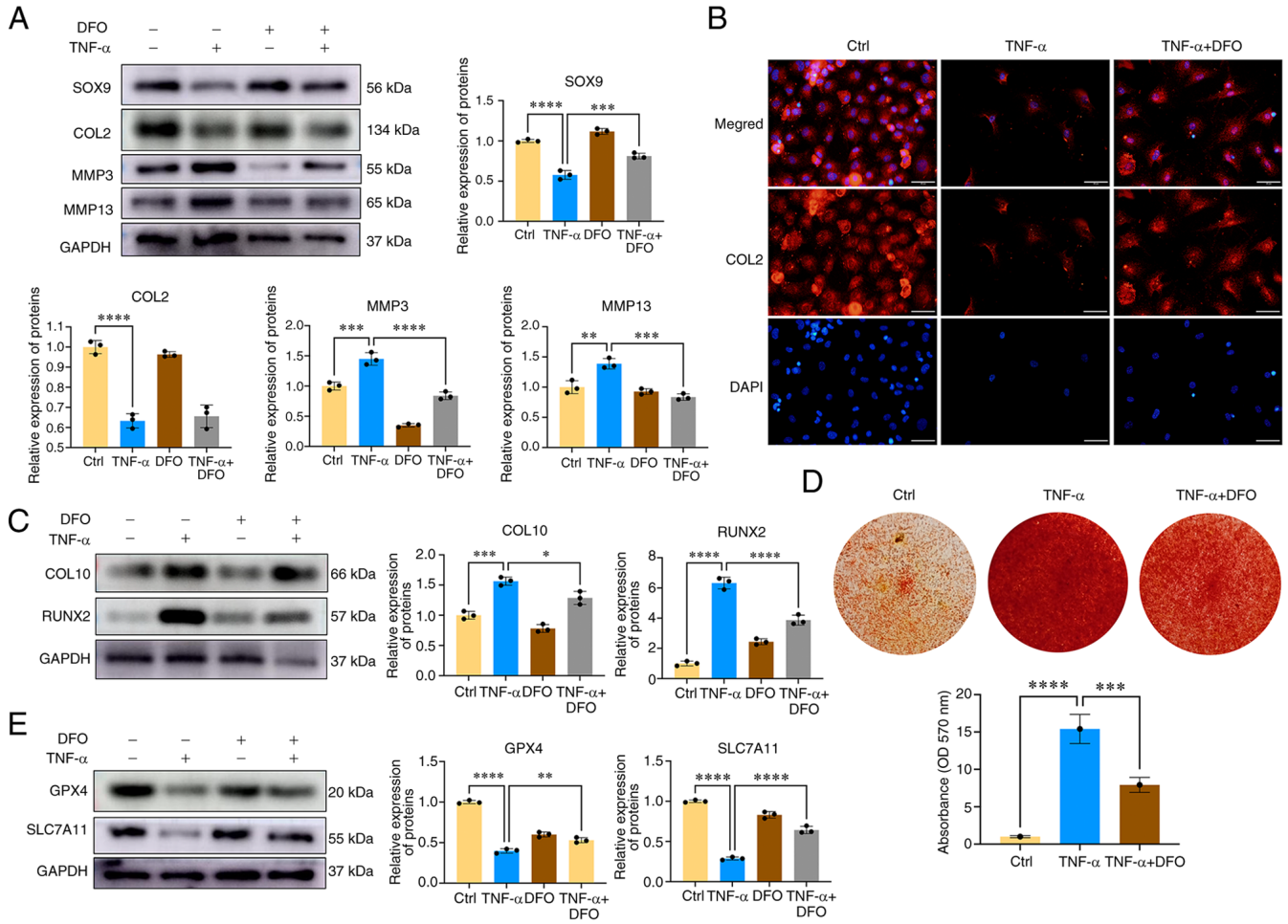

Figure 6. Iron chelation with DFO ameliorates CEP chondrocyte degeneration and calcification. (A) CEP chondrocytes were treated with TNF-α with or without 100 μM DFO for 24 h. Western blotting was conducted to examine the protein expression levels of SOX9, COL2, MMP3, MMP13 and GAPDH. The band density was semi-quantified and normalized to the control. (B) CEP chondrocytes were treated with TNF-α with or without 100 μM DFO. Representative fluorescence photomicrographs of COL2 in CEP chondrocytes are shown. Scale bar, 20 μm. (C) CEP chondrocytes were treated with TNF-α with or without 100 μM DFO for 24 h. Western blotting was conducted to examine the protein expression levels of COL10, RUNX2 and GAPDH. The band density was semi-quantified and normalized to the control. (D) Alizarin Red staining for calcium deposition in CEP chondrocytes. Semi-quantitative analysis of the mineralized nodule in CEP chondrocytes is shown. (E) CEP chondrocytes were treated with TNF-α with or without 100 μM DFO for 24 h. Western blotting was conducted to examine the protein expression levels of GPX4, SLC7A11 and GAPDH. The band density was semi-quantified and normalized to the control. Data are presented as the mean ± SD from three independent experiments. *P<0.05, **P<0.01, ***P<0.001, ****P<0.0001. CEP, cartilage endplate; COL, collagen; Ctrl, control; DFO, desferoxamine; GPX4, glutathione peroxidase 4; MMP, matrix metalloproteinase; SLC7A11, solute carrier family 7 member 11.

been reported that Nrf2 has a protective role in inhibiting IDD development (28). In addition, ferroptosis is a newly identified cell death process that has been shown to serve an important role in NP degeneration (17). In view of the close relationship between ferroptosis and cellular oxidation levels, the roles of Nrf2 signaling were examined with regard to the regulation of CEP chondrocyte ferroptosis and its contribution to the development of IDD in the present study. The results showed that Nrf2 serves important roles in ameliorating CEP degeneration. In addition, Nrf2 can maintain CEP chondrocyte redox homeostasis and mitochondrial function, decrease the levels of Fe^{2+} of the LIP and inhibit ferroptosis by inhibiting NCOA4-mediated ferritinophagy.

In the present study, CEP chondrocytes were treated with TNF-α to mimic endplate osteochondritis. Notably, aging is the leading cause of IDD (19). The results of the present study demonstrated that Nrf2 expression in the CEP was increased at the early stage of the IDD process, and was decreased following 3 months of IDD development. No significant differences in Nrf2 expression levels were observed in the CEP between 16-month-old mice and 1-month-old mice. Similar results were observed in the *in vitro* experiments of the present study. Along with the decrease in Nrf2 expression, decreased Parkin protein expression and increased mitochondrial dysfunction were observed following treatment of the cells with a high concentration of TNF-α treatment. To elucidate the role of Nrf2 in CEP degeneration, CEP chondrocytes were isolated and transfected with Nrf2 siRNA. The data indicated that inhibition of Nrf2 expression promoted CEP degeneration and calcification. Furthermore, inhibition of Nrf2 promoted CEP chondrocyte ferroptosis. The results were consistent with those of the previous study indicating that pro-inflammatory cytokines, such as IL-1β and TNF-α, or oxidative stress could promote Nrf2 expression and activate the antioxidant system (12,13). The results of the present study further indicated that Nrf2 expression in the CEP was decreased in the late stages of IDD, and inadequate activation of the Nrf2 signaling pathway aggravated CEP degeneration via promoting mitochondrial dysfunction and oxidative stress.

Epidemiological evidence has suggested that due to the lack of effective ways for the body to excrete iron, middle-aged and elderly individuals are generally in an iron overload state (29). Previous research has found that when estrogen levels in postmenopausal women decrease by 90% compared with normal levels, serum iron can rapidly increase by 2-3 fold. In addition, the average serum iron level in middle-aged and elderly men is 121 ng/ml, which is considered to be 3-4 fold higher than that noted in adolescents (30,31). Ferroptosis is closely regulated by the lipid repair system, including GSH and GPX4. Two main induction modes of cell ferroptosis have been proposed as follows: One is the classical ferroptosis mode caused by decrease of the GPX4 lipid repair system, and the other is the LIP caused by the increase of cellular Fe^{2+} (32). Increased levels of Fe^{2+} in the LIP can increase sensitivity to ferroptosis (33). The present results indicated that TNF-α increased the concentration of Fe^{2+} in CEP chondrocytes and promoted CEP chondrocyte ferroptosis.

Ferroptosis depends on the imbalance of iron metabolism and the deposition of iron ions in cells. Cellular iron overload can affect the sensitivity of cells to ferroptosis by increasing the concentration levels of iron ions in cells and the levels of lipid peroxidation (34). Numerous diseases and pathological conditions in the human body are attributed to iron overload and ferroptosis, such as chronic renal failure, Parkinson's disease, Alzheimer's disease, osteoporosis and arteriosclerosis (35). In the present study, DFO was used to chelate the cellular iron ions and decrease the Fe^{2+} of the LIP. The data indicated that DFO could inhibit TNF-α-induced CEP degeneration and ferroptosis, and demonstrated that targeting iron metabolism and ferroptosis is a promising treatment strategy for IDD.

Cellular iron homeostasis is achieved by precise regulation of iron metabolism-related proteins involved in iron uptake (transferrin receptor protein 1, divalent metal transporter 1), storage (ferritin) and output [ferroportin (FPN)] (30). Previous studies have indicated that Nrf2 can regulate the iron efflux protein FPN and promote cellular iron output (36). In the present study, it was revealed that, in addition to controlling cellular iron output, Nrf2 could directly regulate the LIP by controlling ferritin synthesis. NCOA4 serves as a specific cargo receptor responsible for facilitating the autophagic degradation of ferritin within lysosomes. This recycling mechanism is commonly referred to as ferritinophagy (37). It has been demonstrated that smoke exposure can promote the expression of NCOA4 in bronchial epithelial cells, which could activate autophagic degradation of ferritin and increase the intracellular LIP (38). The present study demonstrated that Nrf2 could inhibit NCOA4-mediated ferritinophagy, thus decreasing the levels of active Fe^{2+} of the LIP. By contrast, Nrf2 inhibition promoted NOCA4 expression and increased the induction of ferritinophagy, which could increase the levels of cellular free Fe^{2+} and enhance cell susceptibility to ferroptotic cell death.

Parkin-mediated mitophagy serves important roles in NP degeneration and has been demonstrated to be a potential therapeutic target for IDD (25). However, the role of Parkin in CEP degeneration and calcification has been rarely reported (30). The present study demonstrated that the protein expression levels of Parkin were increased in response to a low concentration of TNF-α treatment and were decreased along with the knockdown of Nrf2. Obvious Parkin expression was observed in the control group and peak levels of Parkin expression were observed in response to 1 ng/ml TNF-α; the protein expression levels of Parkin began to decrease when the concentration of TNF-α reached 5 ng/ml. It was hypothesized that this may be because incubation with 5 ng/ml TNF-α for 24 h mimics the pathological condition of OA and begins to cause damage to CEP chondrocytes. A link between the Nrf2 signaling pathway and Parkin protein has previously been demonstrated (29). To investigate the regulation of the Parkin protein by Nrf2, Nrf2 siRNA was synthesized and transfected into CEP chondrocytes. Notably, the expression levels of Parkin were low in the group transfected with scrambled siRNA but were significantly increased by 5 ng/ml TNF-α; it was hypothesized that this may be attributed to the effect of the scrambled siRNA and Lipofectamine on cell viability. The data indicated that the Parkin-mediated mitophagic process was inhibited and mitochondrial morphology destruction was increased with the elevated expression of mitochondrial fission proteins, Drp1, MFF and FIS1. Increased short and granulated mitochondria were observed following inhibition of Nrf2 expression, indicating the destruction and dysfunction of mitochondrial morphology.

In conclusion, the findings of the present study demonstrated the essential role of Nrf2 in controlling CEP degeneration and revealed that Nrf2 could regulate iron homeostasis via NCOA4-mediated ferritinophagy. Inhibition of Nrf2 expression could promote NCOA4-mediated ferritinophagy, thus enhancing the free LIP, and promoting CEP chondrocyte oxidative stress and ferroptotic cell death. Activation of Nrf2 and targeting iron metabolism may be promising strategies for the treatment of IDD.

Acknowledgements

Not applicable.

Funding

The present study was supported by the National Natural Science Foundation of China (grant no. 82002325), the Natural Science Foundation of Shandong Province (grant nos. ZR2020QH075 and ZR2022LZY001), the Shandong Province Traditional Chinese Medicine Science and Technology Project (grant no. M-2022133) and the Shandong Medical and Health Science and Technology Development Plan Project (grant no. 202004071188).

Availability of data and materials

The datasets used and/or analyzed during the current study are available from the corresponding author on reasonable request.

Authors' contributions

XZJ, CS and ZKM contributed to the research conception and design. ZKM, HL, XMF, JHL, QZ and YDS performed the experiments. XZJ, CS, YDS, TD and XDG performed data analysis. ZKM and XZJ drafted the manuscript. XZJ, YDS and CS confirm the authenticity of all the raw data. All authors read and approved the final manuscript.

Ethics approval and consent to participate

All animal protocols were approved by the Institutional Animal Care Committee of the Shandong Provincial Hospital Affiliated to Shandong First Medical University (approval no. 2022-816).

Patient consent for publication

Not applicable.

Competing interests

The authors declare that they have no competing interests.

References

1. Kos N, Gradisnik L and Velnar T: A brief review of the degenerative intervertebral disc disease. Med Arch 73: 421-424, 2019.
2. Dowdell J, Erwin M, Choma T, Vaccaro A, Iatridis J and Cho SK: Intervertebral disk degeneration and repair. Neurosurgery 80 (3S): S46-S54, 2017.
3. Zhong R, Wei F, Wang L, Cui S, Chen N, Liu S and Zou X: The effects of intervertebral disc degeneration combined with osteoporosis on vascularization and microarchitecture of the endplate in rhesus monkeys. Eur Spine J 25: 2705-2715, 2016.
4. Li FC, Zhang N, Chen WS and Chen QX: Endplate degeneration may be the origination of the vacuum phenomenon in intervertebral discs. Med Hypotheses 75: 169-171, 2010.
5. Ashinsky BG, Bonnevie ED, Mandalapu SA, Pickup S, Wang C, Han L, Mauck RL, Smith HE and Gullbrand SE: Intervertebral disc degeneration is associated with aberrant endplate remodeling and reduced small molecule transport. J Bone Miner Res 35: 1572-1581, 2020.
6. Ding Y, Jiang J, Zhou J, Wu X, Huang Z, Chen J and Zhu Q: The effects of osteoporosis and disc degeneration on vertebral cartilage endplate lesions in rats. Eur Spine J 23: 1848-1855, 2014.
7. Zhang X, Yu Y, Lei H, Cai Y, Shen J, Zhu P, He Q and Zhao M: The Nrf-2/HO-1 Signaling Axis: A ray of hope in cardiovascular diseases. Cardiol Res Pract 2020: 5695723, 2020.
8. He F, Ru X and Wen T: NRF2, a transcription factor for stress response and beyond. Int J Mol Sci 21: 4777, 2020.
9. Yang G, Liu X, Jing X, Wang J, Wang H, Chen F, Wang W, Shao Y and Cui X: Astaxanthin suppresses oxidative stress and calcification in vertebral cartilage endplate via activating Nrf-2/HO-1 signaling pathway. Int Immunopharmacol 119: 110159, 2023.
10. Shao Y, Sun L, Yang G, Wang W, Liu X, Du T, Chen F, Jing X and Cui X: Icariin protects vertebral endplate chondrocytes against apoptosis and degeneration via activating Nrf-2/HO-1 pathway. Front Pharmacol 13: 937502, 2022.
11. Xiang Q, Zhao Y, Lin J, Jiang S and Li W: The Nrf2 antioxidant defense system in intervertebral disc degeneration: Molecular insights. Exp Mol Med 54: 1067-1075, 2022.
12. Stockwell BR, Friedmann Angeli JP, Bayir H, Bush AI, Conrad M, Dixon SJ, Fulda S, Gascon S, Hatzios SK, Kagan VE, *et al*: Ferroptosis: A regulated cell death nexus linking metabolism, redox biology, and disease. Cell 171: 273-285, 2017.
13. Galaris D, Barbouti A and Pantopoulos K: Iron homeostasis and oxidative stress: An intimate relationship. Biochim Biophys Acta Mol Cell Res 1866: 118535, 2019.
14. Zeidan RS, Han SM, Leeuwenburgh C and Xiao R: Iron homeostasis and organismal aging. Ageing Res Rev 72: 101510, 2021.
15. Jing X, Lin J, Du T, Jiang Z, Li T, Wang G, Liu X, Cui X and Sun K: Iron Overload is associated with accelerated progression of osteoarthritis: The role of DMT1 mediated iron homeostasis. Front Cell Dev Biol 8: 594509, 2020.
16. Jing X, Du T, Li T, Yang X, Wang G, Liu X, Jiang Z and Cui X: The detrimental effect of iron on OA chondrocytes: Importance of pro-inflammatory cytokines induced iron influx and oxidative stress. J Cell Mol Med 25: 5671-5680, 2021.
17. Yang RZ, Xu WN, Zheng HL, Zheng XF, Li B, Jiang LS and Jiang SD: Involvement of oxidative stress-induced annulus fibrosus cell and nucleus pulposus cell ferroptosis in intervertebral disc degeneration pathogenesis. J Cell Physiol 236: 2725-2739, 2021.
18. Yao X, Sun K, Yu S, Luo J, Guo J, Lin J, Wang G, Guo Z, Ye Y and Guo F: Chondrocyte ferroptosis contribute to the progression of osteoarthritis. J Orthop Translat 27: 33-43, 2020.
19. Wang F, Cai F, Shi R, Wang XH and Wu XT: Aging and age related stresses: A senescence mechanism of intervertebral disc degeneration. Osteoarthritis Cartilage 24: 398-408, 2016.
20. Tang Z, Hu B, Zang F, Wang J, Zhang X and Chen H: Nrf2 drives oxidative stress-induced autophagy in nucleus pulposus cells via a Keap1/Nrf2/p62 feedback loop to protect intervertebral disc from degeneration. Cell Death Dis 10: 510, 2019.
21. Zhang Y, Han S, Kong M, Tu Q, Zhang L and Ma X: Single-cell RNA-seq analysis identifies unique chondrocyte subsets and reveals involvement of ferroptosis in human intervertebral disc degeneration. Osteoarthritis Cartilage 29: 1324-1334, 2021.
22. Santana-Codina N, Gikandi A and Mancias JD: The Role of NCOA4-Mediated ferritinophagy in ferroptosis. Adv Exp Med Biol 1301: 41-57, 2021.
23. Wang W, Jing X, Du T, Ren J, Liu X, Chen F, Shao Y, Sun S, Yang G and Cui X: Iron overload promotes intervertebral disc degeneration via inducing oxidative stress and ferroptosis in endplate chondrocytes. Free Radic Biol Med 190: 234-246, 2022.
24. Song Y, Lu S, Geng W, Feng X, Luo R, Li G and Yang C: Mitochondrial quality control in intervertebral disc degeneration. Exp Mol Med 53: 1124-1133, 2021.
25. Zhang Z, Xu T, Chen J, Shao Z, Wang K, Yan Y, Wu C, Lin J, Wang H, Gao W, *et al*: Parkin-mediated mitophagy as a potential therapeutic target for intervertebral disc degeneration. Cell Death Dis 9: 980, 2018.
26. Ariga K, Miyamoto S, Nakase T, Okuda S, Meng W, Yonenobu K and Yoshikawa H: The relationship between apoptosis of endplate chondrocytes and aging and degeneration of the intervertebral disc. Spine (Phila Pa 1976) 26: 2414-2420, 2001.
27. Vergroesen PP, Kingma I, Emanuel KS, Hoogendoorn RJ, Welting TJ, van Royen BJ, van Dieën JH and Smit TH: Mechanics and biology in intervertebral disc degeneration: A vicious circle. Osteoarthritis Cartilage 23: 1057-1070, 2015.
28. Kang L, Liu S, Li J, Tian Y, Xue Y and Liu X: Parkin and Nrf2 prevent oxidative stress-induced apoptosis in intervertebral endplate chondrocytes via inducing mitophagy and anti-oxidant defenses. Life Sci 243: 117244, 2020.
29. Gozzelino R and Arosio P: Iron homeostasis in health and disease. Int J Mol Sci 17: 130, 2016.
30. Anderson CP, Shen M, Eisenstein RS and Leibold EA: Mammalian iron metabolism and its control by iron regulatory proteins. Biochim Biophys Acta 1823: 1468-1483, 2012.
31. Masaldan S, Clatworthy SAS, Gamell C, Meggyesy PM, Rigopoulos AT, Haupt S, Haupt Y, Denoyer D, Adlard PA, Bush AI and Cater MA: Iron accumulation in senescent cells is coupled with impaired ferritinophagy and inhibition of ferroptosis. Redox Biol 14: 100-115, 2018.
32. Dixon SJ, Lemberg KM, Lamprecht MR, Skouta R, Zaitsev EM, Gleason CE, Patel DN, Bauer AJ, Cantley AM, Yang WS, *et al*: Ferroptosis: An iron-dependent form of nonapoptotic cell death. Cell 149: 1060-1072, 2012.
33. Li J, Cao F, Yin HL, Huang ZJ, Lin ZT, Mao N, Sun B and Wang G: Ferroptosis: Past, present and future. Cell Death Dis 11: 88, 2020.
34. Xie Y, Hou W, Song X, Yu Y, Huang J, Sun X, Kang R and Tang D: Ferroptosis: Process and function. Cell Death Differ 23: 369-379, 2016.
35. Siddique A and Kowdley KV: Review article: The iron overload syndromes. Aliment Pharmacol Ther 35: 876-893, 2012.
36. Han K, Jin X, Guo X, Cao G, Tian S, Song Y, Zuo Y, Yu P, Gao G and Chang YZ: Nrf2 knockout altered brain iron deposition and mitigated age-related motor dysfunction in aging mice. Free Radic Biol Med 162: 592-602, 2021.
37. Santana-Codina N and Mancias JD: The role of NCOA4-Mediated ferritinophagy in health and disease. Pharmaceuticals (Basel) 11: 114, 2018.
38. Zi Y, Wang X, Zi Y, Yu H, Lan Y, Fan Y, Ren C, Liao K and Chen H: Cigarette smoke induces the ROS accumulation and iNOS activation through deactivation of Nrf-2/SIRT3 axis to mediate the human bronchial epithelium ferroptosis. Free Radic Biol Med 200: 73-86, 2023.